pubs.acs.org/acschemicalbiology

Letter

# Enhanced EphB2-Specific Peptide Inhibitors through Stabilization of Polyproline II Helical Structure

Jessica C. Tennett, Sophie R. Epstein, and Nicholas Sawyer*

Cite This: *ACS Chem. Biol.* 2024, 19, 1214−1221

Read Online

ACCESS | Metrics & More | Article Recommendations | Supporting Information



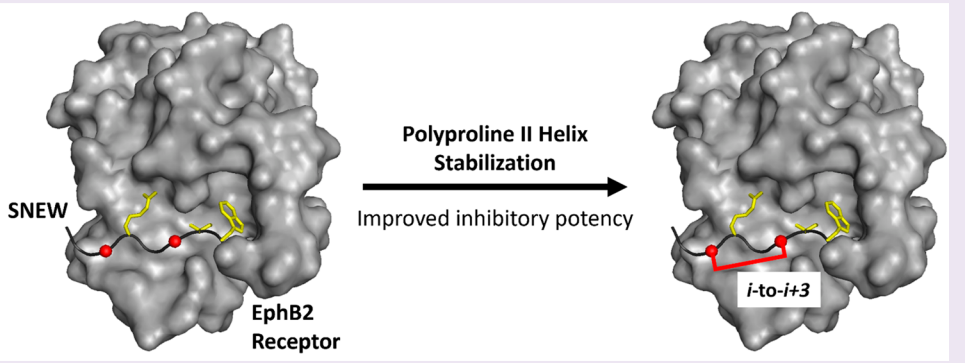


**ABSTRACT:** Ephrin (Eph) receptors are the largest family of receptor tyrosine kinases. Interactions between Eph receptors and their membrane-bound ephrin protein ligands are associated with many developmental processes as well as various cancers and neurodegenerative diseases. With significant crosstalk between different Eph receptors and ephrin ligands, there is an urgent need for high-affinity ligands that bind specifically to individual Eph receptors to interrogate and modulate their functions. Here, we describe the rational development of potent EphB2 receptor inhibitors derived from the EphB2 receptor-specific SNEW peptide. To improve inhibitory potency, we evaluated 20+ cross-linkers with the goal of spanning and stabilizing a single polyproline II helical turn observed when SNEW binds to the EphB2 receptor. Of the cross-linkers evaluated, an 11-atom cross-linker, composed of a rigid 2,7-dimethylnaphthyl moiety between two cysteine residues, was found to yield the most potent inhibitor. Analysis of the cyclized region of this peptide by NMR and molecular dynamics simulations suggests that cross-linking stabilizes the receptor-bound polyproline II helix structure observed in the receptor−peptide complex. Cross-linked SNEW variants retained binding specificity for EphB2 and showed cross-linker-dependent resistance to trypsin proteolysis. Beyond the discovery of more potent EphB2 receptor inhibitors, these studies illustrate a novel cyclization approach with potential to stabilize polyproline II helical structure in various peptides for specific targeting of the myriad protein−protein interactions (PPIs) mediated by polyproline II helices.

## INTRODUCTION

Ephrin (Eph) receptors represent the largest receptor tyrosine kinase family.[1] In humans, there are 14 Eph receptors divided into two subclasses based on their preferential binding to distinct subclasses of membrane-bound ephrin protein ligands.[2,3] Interactions between Eph receptors and ephrins are implicated in a wide array of physiological and pathological processes, including embryonic development, cell migration, and cancer.[3−6] Eph receptor−ephrin interactions are promiscuous, in that each Eph receptor can bind with high affinity to many different ephrins, and each ephrin can bind to many different Eph receptors.[7,8] Thus, understanding the behavior of individual Eph receptors and developing targeted therapeutic strategies is challenging.[9,10]

One approach to modulating individual Eph receptor function is to identify novel molecules that target specific Eph receptors. Specific peptide ligands for the EphA2, EphA4, EphB2, and EphB4 receptors have been identified by artificial selection using phage display and biochemical/structural characterization, including both agonists and antagonists.[11−14] These molecules serve as tools for probing the function of specific target Eph receptors.

Here, we describe a rational approach to improve the inhibitory potency of one such molecule, the EphB2-specific peptide SNEW.[13] The core principle of our approach was to introduce a cross-linker to stabilize the receptor-bound peptide structure in a similar fashion to previous studies.[15−17] Specifically, we sought to stabilize the polyproline II helix

Received: December 21, 2023
Revised: May 6, 2024
Accepted: May 7, 2024
Published: May 13, 2024




https://doi.org/10.1021/acschembio.3c00791
*ACS Chem. Biol.* 2024, 19, 1214−1221

structure at the C-terminus of SNEW. Factors influencing polyproline II helix stability have been studied extensively in proline-rich peptides, including several examples of cross-linking.[18−24] Complementary to these studies, we used the wealth of existing knowledge about cross-linking of peptide α-helices to rationally guide the screening of cross-linkers for stabilization of a single turn of the C-terminal polyproline II helical segment of SNEW.[25] Through design, synthesis, and evaluation of a collection of SNEW variants, we identified variants that are more potent than SNEW in inhibiting the EphB2−ephrin B2 interaction. NMR analysis of the cross-linked region from the most potent variant supports the hypothesis that cross-linking stabilizes the polyproline II helix structure as desired. We also found that cross-linked variants retained binding specificity for the EphB2 receptor and exhibited cross-linker-dependent resistance to trypsin proteolysis. Importantly, these studies provide a new synthetic approach to cyclize and stabilize polyproline II helical segments for broader targeting of protein−protein interactions beyond the EphB2 receptor.[26−28]

## RESULTS AND DISCUSSION

Starting from the amino acid sequence of SNEW (SNEWIQPRLPQH) and its structure bound to the EphB2 receptor,[13,14] we first sought to understand the contributions of individual amino acid residues to the EphB2 binding interaction to guide cross-linker design (Figure 1A). We performed computational alanine scanning[29] and observed that (1) Trp4 and Ile5 are predicted to be the most significant hotspots, (2) Gln6 and Leu9 make minimal contributions to the binding interaction, and (3) the C-terminal histidine is absent in both copies of the crystallized complex (Figure S1A). Based on these observations, we initially synthesized, purified, and evaluated three peptides: SNEW (**1**), SNEW-AA (**2**, SNEAAQPRLPQH, both Trp4 and Ile5 substituted with Ala), and SNEWΔH (**3**, SNEWIQPRLPQ, missing the C-terminal histidine).

Evaluation of peptide inhibitory potency against the EphB2 receptor−ephrin B2 interaction led us to identify peptide **3** as a suitable context for cross-linker evaluation. We conducted enzyme-linked immunosorbent assays (ELISAs), similar to those previously described, and found that inhibition of the EphB2 receptor−ephrin B2 interaction by SNEW (peptide **1**) was similar to prior reports ($IC_{50}$ ∼ 10 μM, Figure S1B).[13] Minimal inhibition was observed even at the highest peptide concentration of 250 μM tested for peptide **2**, which is consistent with Trp4 and Ile5 as interaction hotspots. The $IC_{50}$ value for peptide **3** was similar to peptide **1** (∼15 μM), suggesting that the C-terminal histidine plays little to no role in binding to the EphB2 receptor, as predicted by computational alanine scanning. Synthetic yields were significantly lower for peptide **1** compared to peptide **3**, so all additional variants were based on peptide **3**.

Next, we used data from existing α-helical cross-linkers to guide the cross-linker design for a single polyproline II helix turn. We adopted this approach because all helices, by definition, have a repeating unit that results in regular, periodic alignment of amino acid residues on the same side of the helix at a defined distance. Thus, even in the absence of a robust approach to cross-link and stabilize polyproline II helices,[23,24] we were able to draw upon the large number of cross-linkers evaluated for peptide α-helices across one, two, or three turns of the α-helix (Figure S2).[25,30−35] Analysis of the relationship

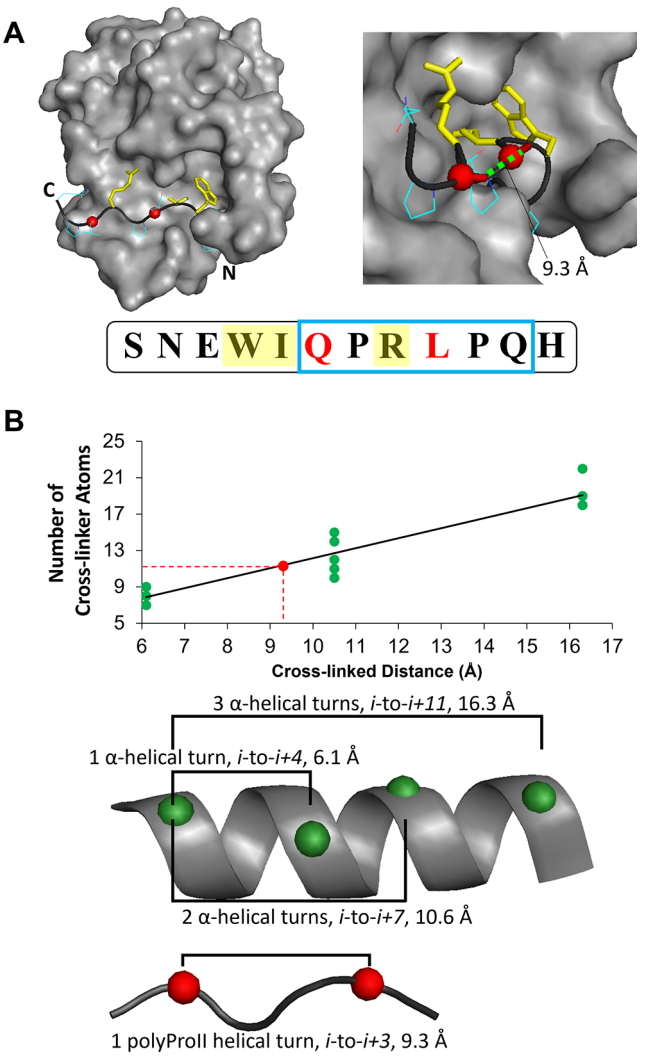


**Figure 1.** Design approach for stabilizing the EphB2 receptor-bound structure of SNEW. (A) Computational alanine scanning identified three interaction hotspots (yellow: Trp4, Ile5, Arg8). Noninteracting residues (red) with an *i*-to-*i*+3 spacing are suitable for cross-linking to stabilize a single turn within the polyproline II helix region of SNEW (outlined in blue). (B) Analysis of α-helical cross-linkers spanning one, two, or three helical turns (green data points with helical pitches of 6.1, 10.6, and 16.3 Å, respectively; cross-linker structures illustrated in the Supporting Information) revealed a correlation between cross-linked distance and number of cross-linker atoms (black). Interpolation to the 9.3 Å pitch for a single polyproline II helix turn suggests an 11-atom cross-linker as optimal to stabilize a single polyproline II helix turn (red). Cartoon representations of cross-linked distances are provided below the plot.

between the cross-linked distance and the number of cross-linker atoms suggested a linear correlation (Figure 1B). Interpolating from the line of best fit using a helical pitch of 9.3 Å for a single polyproline II helix turn between residues *i* and *i*+3,[23,36,37] we hypothesized that an 11-atom cross-linker would serve as a productive starting point to identify cross-linkers that stabilize the polyproline II helix.

Based on this information, we initially synthesized six SNEW variants with different 11-atom cross-linkers. All cross-linkers were introduced by substitution of Gln6 and Leu9 (e.g., SNEWI$X_1$PR$X_2$PQ with cross-linking between $X_1$ and $X_2$, Figure 2A). These residues are at an *i*-to-*i*+3 spacing to span a


https://doi.org/10.1021/acschembio.3c00791
ACS Chem. Biol. 2024, 19, 1214−1221

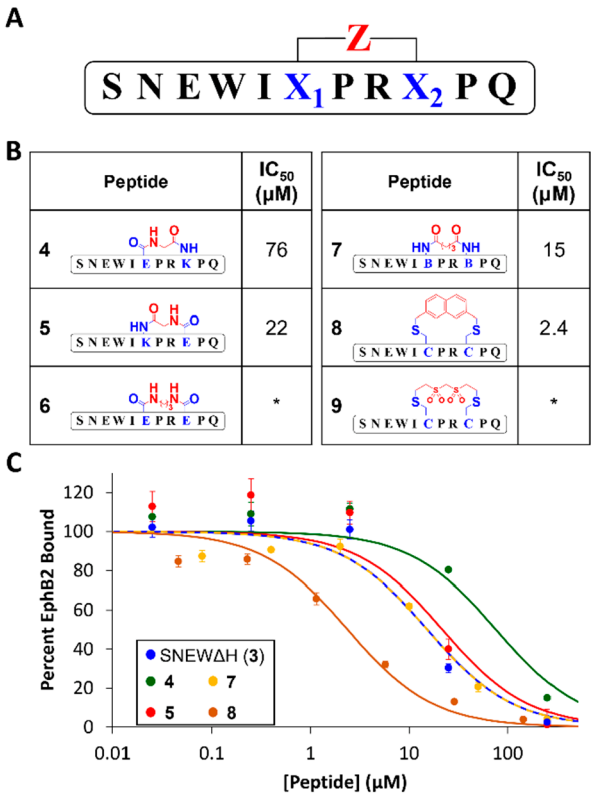


**Figure 2.** Inhibition of the EphB2 receptor−ephrin B2 receptor interaction by SNEW variants with 11-atom cross-linkers. (A) General diagram of cross-linked SNEW variants. (B) Cross-linked SNEW variants and $IC_{50}$ values. *Unable to estimate $IC_{50}$ value. (C) ELISA data for inhibition of the EphB2 receptor−ephrin B2 interaction by **3**−**5**, **7**, and **8**. ELISA data for all SNEW variants are included in the Supporting Information (Figure S7).

single polyproline II helix turn and were previously predicted to contribute minimally to the SNEW−EphB2 receptor interaction. Prior studies have indicated that functional group identity and placement within peptide cross-linkers can dramatically impact stabilization of a desired structure,[30,31] leading us to investigate four lactam cross-linked and two cysteine cross-linked SNEW variants (Figure 2B). We chose lactamization and cysteine cross-linking because of their widespread use, operational simplicity for peptide cross-linking, and wide array of commercially available reagents.[17,30] Two of the lactam variants (**4**, **5**) were synthesized by bridging Lys and Glu side-chains with an intervening glycine residue, differing only in the relative placement of the Lys and Glu residues in the peptide (Figure S3). A third lactam variant (**6**) was synthesized by cross-linking two Glu residues with 1,3-diaminopropane (Figure S4). A fourth lactam variant (**7**) was synthesized by cross-linking two L-2,4-diaminobutryic acid (Dab) residues using glutaric anhydride (Figure S5). The two remaining variants were formed by alkylation of a bisthiol SNEW variant (SNEWICPRCPQ) with either 2,7-bis-(bromomethyl)naphthalene (**8**) or bis(vinylsulfonyl)methane (**9**, Figure S6). These cross-linkers represent a subset of all possible 11-atom lactam and cysteine cross-linked variants. For lactam variants, we intentionally avoided Asp-containing cross-linkers because amino acids with short, polar side chains (e.g., Asp, Asn, Ser, Thr) have been reported to destabilize polyproline II helices.[20] Attempts to cross-link L-ornithine residues with malonic acid derivatives led to decomposition during malonic acid coupling.[38] For cysteine cross-linking, allylic and benzyl bromides, as well as vinyl sulfones, are most commonly used because they react with cysteines chemoselectively under mild reaction conditions.[17,39] Bis-(vinylsulfonyl)methane and 2,7-bis(bromomethyl)naphthalene were selected as commercially available reagents that fall within this scope to yield 11-atom cross-linkers.

Screening of all six variants by ELISA revealed that the naphthyl cross-linked variant **8** had the highest inhibitory potency, i.e., lowest $IC_{50}$ value. The inhibitory potency of variant **8** was ∼2−3 $\mu$M, which is at least a 4-fold improvement compared to peptides **1** and **3** (Figure 2C). In contrast, the inhibitory potencies of peptides **5** and **7** were similar to **3** ($IC_{50}$ = 15−22 $\mu$M) while the inhibitory potencies of peptides **6** and **9** could not be accurately quantified up to $IC_{50}$ values of 250 $\mu$M (Figure S7). Peptides **4** and **5**, which differ only in the placement of cross-linker Glu and Lys residues, displayed very different inhibitory potencies of 76 and 22 $\mu$M, respectively, emphasizing the importance of functional group placement in peptide cross-linkers.[30] To rule out the hypothesis that the potency of variant **8** was due to an overall increase in the peptide's hydrophobic character, we also prepared and evaluated variant **10** in which each cysteine is modified with a benzyl group. This variant has similar hydrophobic character to peptide **8** without cross-linking between cysteines. Variant **10** displayed a potency of approximately 50−60 $\mu$M, significantly lower than both peptides **3** and **8** (Figure S7), suggesting that variant **8**'s potency is derived from cross-linking and not solely increased hydrophobic character. Overall, these data suggest that the naphthyl cross-linker's size and rigidity are important factors in increasing inhibitory potency.

Because we observed wide variation in inhibitory potency for SNEW variants with 11-atom cross-linkers, we screened fifteen additional SNEW variants with cross-linkers ranging from 7 to 14 atoms (Figure 3, Table S2). For lactam cross-linked peptides, we focused on seven variants related to the two 11-atom cross-linker variants with the lowest $IC_{50}$ values (**5** and **7**). Variants of **5** included (1) direct cross-linking of Lys and Glu at *i* and *i*+3, respectively, which significantly decreased inhibitory potency (**11**, $IC_{50}$ = 47 $\mu$M), (2) replacement of Glu with longer carboxylic acid side chains and direct cross-linking to Lys, which showed length-dependent changes in inhibitory potency with a propionyl cysteine-containing variant showing greater potency than peptide **3** (**13**, $IC_{50}$ = 5.8 $\mu$M), and (3) longer cross-linkers between Lys and Glu ($\beta$-alanine (**14**), $\gamma$-aminobutyric acid (**15**)), which had no effect or slightly improved inhibitory potency compared to peptide **3**, respectively. Variants of **7** included either a shorter succinyl cross-linker (**16**) or more rigid isophthaloyl cross-linker (**17**), both of which decreased inhibitory potency ($IC_{50}$ = 24−40 $\mu$M). Eight additional variants were readily synthesized by cysteine alkylation starting from the same bisthiol SNEW peptide variant using an array of different biselectrophiles. With the exception of the *trans*-2-butenyl cross-linker (**19**, $IC_{50}$ = 7.7 $\mu$M), all variants with cross-linkers shorter than the 2,7-dimethylnaphthyl cross-linker showed significantly decreased inhibitory potencies than peptide **3**. The 2,6-dimethylnaphthyl cross-linked variant **24** showed similar, but slightly lower, inhibitory potency ($IC_{50}$ = 9.1 $\mu$M) compared to the 2,7-dimethylnaphthyl variant **8**. Lastly, the longer 4,4′-dimethyl-1,1′-biphenyl cross-linker produced a variant (**25**) for which inhibitory potency could not be accurately quantified. Overall,


https://doi.org/10.1021/acschembio.3c00791
ACS Chem. Biol. 2024, 19, 1214−1221

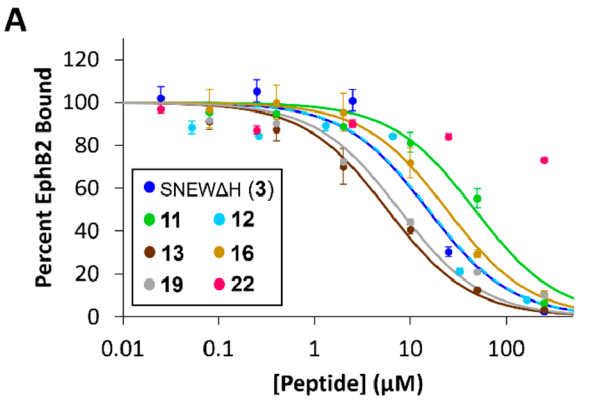


| Peptide | $IC_{50}$ (μM) | Peptide | $IC_{50}$ (μM) |
|---|---|---|---|
| 11 SNEWI K PR E PQ | 47 | 16 SNEWI B PR B PQ | 24 |
| 12 SNEWI K PR C PQ | 16 | 19 SNEWI C PR C PQ | 7.7 |
| 13 SNEWI K PR C PQ | 5.8 | 22 SNEWI C PR C PQ | >250 |

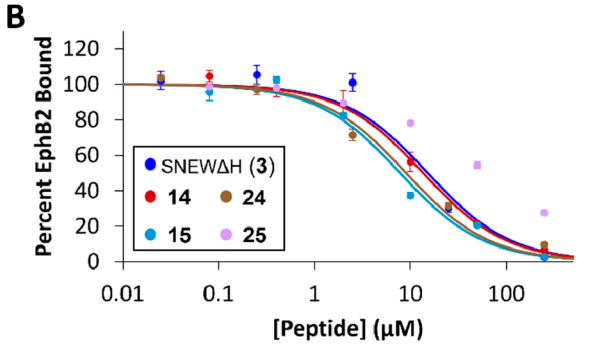


| Peptide | $IC_{50}$ (μM) | Peptide | $IC_{50}$ (μM) |
|---|---|---|---|
| 14 SNEWI K PR E PQ | 14 | 24 SNEWI C PR C PQ | 9.1 |
| 15 SNEWI K PR E PQ | 7.8 | 25 SNEWI C PR C PQ | * |

**Figure 3.** Inhibition of the EphB2 receptor−ephrin B2 interaction by SNEW variants with non-11-atom cross-linkers. (A) ELISA data, peptide structures, and $IC_{50}$ values for selected variants with cross-linkers with fewer than 11 atoms. (B) ELISA data, peptide structures, and $IC_{50}$ values for selected variants with cross-linkers with greater than 11 atoms. *Unable to estimate $IC_{50}$ value. ELISA data for all SNEW variants are included in the Supporting Information (Figure S7).

these data illustrate a lack of correlation between cross-linker length and inhibitory potency (Figure S8) but allowed identification of several variants with greater inhibitory potency than peptide **3**.

To better understand the relationship between structure and inhibitory potency, we first attempted to study peptide variants using CD spectroscopy. Only the C-terminal half of SNEW folds into a polyproline II helix when bound to the EphB2 receptor. For our SNEW variants, we did not observe the weak maximum at 228 nm that is commonly attributed to polyproline II helical structure (Figure S9).[18−22,24] The CD spectrum for the naphthyl cross-linked variant **8** was especially unusual for a peptide, displaying a prominent minimum at 235 nm, a maximum at 218 nm, and a minimum at 200 nm. The 2,6-dimethylnaphthyl cross-linked variant **24** also displayed these minima and maxima, though intensities were smaller at all wavelengths. These minima at 233−236 nm for variants **8** and **24** are reminiscent of previous CD spectra for naphthyl-containing compounds.[40−43] Because these spectral features precluded estimates of relative folding, especially for the most potent variant **8**, we prepared and evaluated several additional naphthyl-containing variants to better understand the likely origins of these CD spectra. Variants **26** (SNEWICPRAPQ) and **27** (SNEWIAPRCPQ) are analogs of variants **8** and **24** in which the cysteine residue is modified with a 2-methylnaphthyl group and the second cysteine of **8** is substituted by alanine to prevent cross-linking (Table S1). These variants did not display minima at 233−236 nm or maxima at 218−222 nm, suggesting that the presence of a 2-methylnaphthyl group in these peptides is insufficient to give rise to the CD spectral features observed for variant **8** (Figure S9F). On the other hand, variants **28** (Ac-GCPRCPGY-$NH_2$) and **29** (Ac-CPRC-$NH_2$), which differ from variant **8** by the flanking sequences around the cyclized CPRC region, display the same CD spectral shape as variant **8**, albeit with lower overall intensities and a 1−2 nm blue shift in their respective maxima (Figure S9F). These data suggest a dominant influence of the cross-linked 2,7-dimethylnaphthyl group on the CD spectrum of variant **8** which may prove to be a useful reference in future studies.

Because CD experiments did not yield significant structural insight, we performed NMR spectroscopy experiments to gain more detailed insight into the relationship between peptide structure and inhibitory potency for the most potent variant **8**. To do so, we examined two simplified peptides, **29** and **30**. Peptide **29**, Ac-CPRC-$NH_2$ with the two cysteine residues cross-linked with the 2,7-dimethylnaphthyl group, reproduces the cyclized region of peptide **8** with a limited number of amide bonds to allow direct measurement of amide $^3J_{NH\alpha}$ coupling constants from the 1D $^1H$ spectrum for estimation of $\varphi$ dihedral angles using the Karplus equation (Figures 4A and S10).[44,45] We found that the average $\varphi$ dihedral angle values for all nonproline residues, calculated from the measured $^3J_{NH\alpha}$ coupling constants, were within 10° of the ideal polyproline II helix $\varphi$ dihedral angle of −75°. We then used both estimated $\varphi$ dihedral angles and NOE's to constrain a molecular dynamics simulation. The 20 lowest-energy structures exhibit high backbone convergence (average RMSD = 0.67 Å), and an overall structure consistent with a polyproline II helix (average distance of 9.0 Å between $\alpha$-carbons at positions $i$ and $i$+3).

As a control, we also collected NMR spectra for peptide **30**, Ac-CPRC-$NH_2$ with one benzyl group on each cysteine, and failed to observe a well-defined structure (Figure S11). Peptide **30** is an analog of peptide **29** with similar hydrophobicity but without cross-linking macrocyclization. Only sequential $i$, $i$+1 NOE's were observed for peptide **30** (in part because benzyl protons were largely indistinguishable). Estimated $\varphi$ dihedral angles from $^3J_{NH\alpha}$ coupling constants were similar to, but slightly lower than, peptide **29** with an average value of −83°. We performed a molecular dynamics simulation of peptide **30**, which, in contrast to simulations with peptide **29**, failed to fully


https://doi.org/10.1021/acschembio.3c00791
ACS Chem. Biol. 2024, 19, 1214−1221

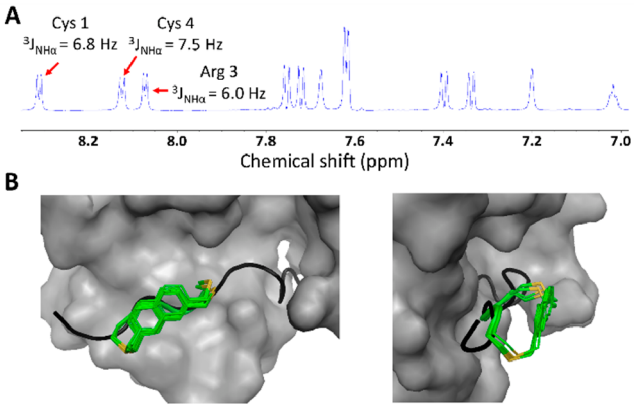


**Figure 4.** Structure model of cyclized region of peptide **8**. (A) $^1$H NMR spectrum for Ac-CPRC-$NH_2$ with a 2,7-dimethylnaphthyl cross-linker between the two cysteines. (B) Overlay of 20 lowest-energy structures from a constrained molecular dynamics simulation of the peptide (green) with the complex between SNEW (black) and the EphB2 receptor (gray). The overlay shows high backbone convergence among the 20 structures, structural similarity with the target region of SNEW (RMSD = 0.67 Å across all C$\alpha$), and orientation of the naphthyl cross-linker away from the receptor surface.

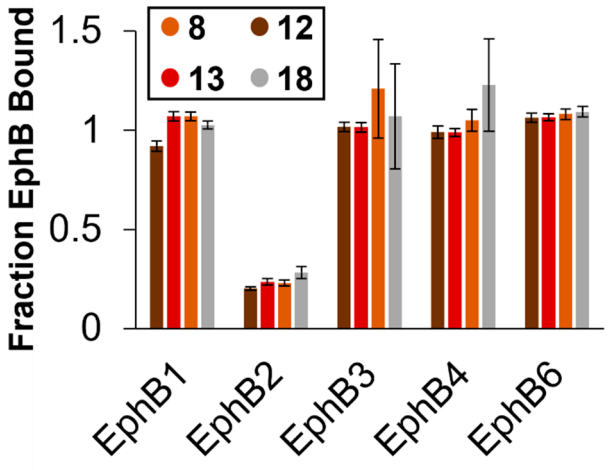


**Figure 5.** Specific inhibition of the EphB2 receptor by cross-linked SNEW variants. ELISA data for inhibition of the interaction between ephrin B2 and the indicated EphB receptor in the presence of 50 $\mu$M of each of the indicated peptides shows ELISA signal reduction for the EphB2 receptor only.

converge on a defined backbone conformation but displayed an overall preference for $3_{10}$ and/or $\alpha$-helical conformations (Figure S12).

Using the data from our molecular dynamics simulations, we performed an overlay of the conformational ensemble of peptide **29** with the analogous region of SNEW in the SNEW–EphB2 receptor complex and found that the naphthyl cross-linker is oriented away from the receptor (Figure 4B). This observation suggests that stabilization of the bound peptide conformation is most likely responsible for the observed increase in inhibitory potency, though we cannot rule out protein dynamics that might result in cross-linker–receptor interaction. Overall, these data suggest that the 2,7-dimethylnaphthyl cross-linker stabilizes a polyproline II helix structure. We also speculate that, given a lack of apparent interaction between the cross-linker and receptor, this cross-linking approach might be applied in an amino acid sequence-independent fashion to stabilize other peptides as polyproline II helices.

Evaluation of EphB2 receptor specificity of the top four most potent cross-linked SNEW variants (**8**, **12**, **13**, **18**) revealed that these cross-linked variants maintain SNEW's specificity for EphB2 (Figure 5). We performed ELISA studies as described earlier but using different EphB receptors (EphB1–4, EphB6). In the presence of 50 $\mu$M of any of the four peptides, only the ELISA signal for the EphB2 receptor decreased, indicating inhibition of only the EphB2 receptor–ephrin B2 interaction. The ELISA signal did not decrease for EphB1, EphB3, EphB4, or EphB6, demonstrating that the SNEW variants do not affect interactions between ephrin B2 and these EphB receptors. Thus, cross-linking does not influence specific binding to the EphB2 receptor, which is consistent with our molecular model showing no cross-linker–receptor interaction.

Lastly, we evaluated proteolytic resistance using trypsin and discovered an unexpected correlation between peptide hydrophobicity and trypsin proteolysis. Trypsin specifically hydrolyzes peptide bonds at the C-terminal end of lysine (K) or arginine (R). We chose trypsin because the single trypsin cleavage site after Arg8 reports directly on the degree to which a cross-linker "shields" the macrocyclized peptide segment from proteolysis. As a baseline, peptide **3** was not significantly digested (approximately 10%) over 4 h, which is somewhat unusual for a linear peptide (Figure S13). In contrast, the linear variant **10**, in which Gln6 and Leu9 were substituted with *S*-benzyl-cysteine, was approximately 70% digested in the same time frame, suggesting a potential relationship between peptide hydrophobicity and trypsin proteolysis. Cross-linking provided some proteolytic resistance for lactam cross-linked variants **4**–**7**, which showed less than 5% digestion within 4 h. However, naphthyl cross-linked variants **8** and **24** showed similar digestion rates to peptide **10**, reinforcing the notion that hydrophobicity, rather than cross-linking, was the dominant factor in determining proteolysis rate, though an intermediate digestion rate for biphenyl cross-linked variant **25** suggests potential influence from peptide conformation as well. Similar to lactam cross-linked variants, the *trans*-2-butenyl cross-linked variant **19** has lower cross-linker hydrophobicity overall and displayed no apparent digestion within 4 h. These data suggest that stability to trypsin proteolysis is independent of EphB2 receptor inhibitory potency. Improvements in proteolytic stability are thus potentially achievable with amide modification, such as N-alkylation or N-amination.[22,46]

In conclusion, we have identified a series of cross-linked EphB2 receptor-specific peptide inhibitors with increased inhibitory potency. Our overall goal was to identify one or more cross-linkers that would stabilize the EphB2 receptor-bound conformation of SNEW, specifically within the peptide's C-terminal polyproline II helix. To guide our approach, we examined a variety of $\alpha$-helix-stabilizing cross-linkers and interpolated from the observed correlation between cross-linked distance and number of cross-linker atoms to suggest a starting point of 11 atoms for cross-linker length to span the 9.3 Å of a single polyproline II helical turn. Surveying a range of cross-linker chemistries, we found that a SNEW variant cross-linked with a rigid 2,7-dimethylnaphthyl cross-linker between two cysteines was the most potent EphB2 receptor inhibitor. Structural analysis suggested that this cross-linker stabilizes the target polyproline II structure without apparent


https://doi.org/10.1021/acschembio.3c00791
ACS Chem. Biol. 2024, 19, 1214–1221

cross-linker−receptor interaction. Thus, we hypothesize that this approach might be applied to other peptides that adopt polyproline II helices in protein−protein interactions,[26,36,47] potentially improving their inhibitory potencies with cross-linking alone or in combination with other approaches to stabilize polyproline II helices.[21,22]

## MATERIALS AND METHODS

**General Information.** Commercially purchased solvents and reagents were used without further purification. Nα-Fmoc-protected amino acids and peptide synthesis reagents were purchased from Advanced ChemTech, ChemImpex International, Oakwood Chemical, Gyros Protein Technologies, and Sigma-Aldrich. Peptides were synthesized manually or using a Gyros Protein Technologies PurePep Chorus synthesizer with peptide coupling reactions performed at 55 °C. Peptides were purified on preparative $C_{18}$ columns using reverse-phase high-performance liquid chromatography (RP-HPLC) on a Shimadzu Nexera HPLC system using gradients of water and acetonitrile (ACN) containing 0.1% trifluoroacetic acid (TFA). Peptide purity was evaluated by analytical HPLC using a Luna 5 μm C18(2) column (150 × 4.6 mm) on an Agilent 1100 HPLC system with a flow rate of 0.3 mL/min (gradient: 5−95% solvent B over 30 min, solvent A = 0.1% TFA, B = 95% ACN, 5% water, 0.1% TFA; Figure S14). High-resolution mass spectrometry data were collected on a Shimadzu MALDI-8020 Benchtop MALDI-TOF mass spectrometer using α-cyano-4-hydroxycinnamic acid as the matrix. Mass spectrometry grade trypsin was purchased from Fisher Scientific (PI90057). Recombinant proteins were purchased as follows: hexahistidine-tagged mouse ephrin B2 from Sino Biological (50598-M08H), rat EphB1-Fc chimera from Fisher Scientific (1596B1200), human EphB2-Fc chimera from BioLegend (791706), human EphB3-Fc chimera from Fisher Scientific (5667B3050), mouse EphB4-Fc chimera from Fisher Scientific (501622148), human EphB6-Fc chimera from Fisher Scientific (501614286), anti-Fc antibody-alkaline phosphatase conjugate from Sigma-Aldrich (A9544-.5ML). *para*-Nitrophenylphopshate was purchased from Fisher Scientific.

**Peptide Synthesis.** All peptides were synthesized following standard Fmoc solid-phase approaches on Rink MBHA resin except where noted below. All peptides were synthesized on high-loading resin (0.62 mmol/g resin) except in cases of on-resin lactamization. In these cases, low-loading resin (0.31 mmol/g resin) was used.

Manual coupling reactions were performed by reacting 5 mol equiv each of Nα-Fmoc-protected amino acid, ethyl cyanohydroxyiminoacetate (Oxyma), and diisopropylcarbodiimide (DIC) in N,N-dimethylformamide (DMF) for 20−30 min and adding the activated ester to the deprotected peptide. Deprotection of the Fmoc protecting group was carried out by two sequential reactions of 15−20 min each with 20% piperidine in DMF. Between coupling and deprotection reactions, the resin was washed sequentially with dichloromethane (DCM, 3×) and DMF (3×).

Automated peptide synthesis was carried out on a Gyros Protein Technologies PurePep Chorus synthesizer. Dried Rink MBHA resin was swollen for 10 min in DMF before the first deprotection reaction. Coupling reactions were performed using 4 mol equiv each of Nα-Fmoc-protected amino acid, O-(1H-6-chlorobenzotriazole-1-yl)-1,1,3,3-tetramethyluronium hexafluorophosphate (HCTU), and *N*-methylmorpholine (NMM) at 55 °C. Deprotection of the Fmoc protecting group was carried out by two sequential reactions of 15 min each. Between coupling and deprotection reactions, the resin was washed three times with DMF. At the end of peptide synthesis, the Fmoc-protected peptide was washed with DMF (3×) and DCM (4×). Removal of the Fmoc protecting group was performed as described for manual peptide synthesis.

At various points during synthesis, especially during cross-linker assembly, microcleavage reactions were performed by cleaving a small amount of resin with 1 mL of freshly prepared 95% TFA, 2.5% $H_2O$, and 2.5% TIPS for 30 min. After dilution with 3−4 mL of acetonitrile, 1 μL of sample was mixed with 4 μL of saturated α-cyano-4-hydroxycinammic acid (CHCA, prepared in 1:1 acetonitrile/water with 0.1% trifluoroacetic acid). A 1 μL volume of this mixture was added to a stainless steel MALDI plate and analyzed by MALDI.

Synthesis of cross-linked peptides is described in detail in the Supporting Information.

**General Procedure for Competitive EphB2 Receptor−Ephrin B2 ELISA.** For each ELISA, the following stock solutions were prepared immediately before their respective use:

- EphrinB2-6xHis: 12.5 μL of 125 μg/mL ephrinB2-6xHis dissolved in 5 mL of TBST (50 mM Tris, pH 7.50, 150 mM NaCl, 0.01% Tween 20)
- EphB2-Fc: Initially, 1 μL of 1.35 μg/mL EphB2-Fc was dissolved in 1.67 mL of TBST. After mixing, a 250 μL volume of this solution was added to 4.75 mL of TBST to create the EphB2-Fc stock solution
- Antihuman IgG: 1 μL of antihuman IgG (Fc-specific) antibody in 50 mL of TBST
- *para*-Nitrophenyl phosphate (pNPP): 1 mg $mL^{-1}$ in 1× diethanolamine buffer (pH 9.8)

In between steps, all sample volume was removed by pipetting, and each well was washed twice with TBST.

Step 1: In a Ni-coated 96-well plate, a volume of 200 μL of ephrinB2-6xHis stock solution was added to each sample well. The plate was covered with parafilm and incubated for 1 h with mild shaking (150 rpm) on an orbital shaker at RT.

During the incubation step, 5- or 10-fold serial dilutions of peptide were prepared. From a 10 mM peptide stock solution in water, 5-fold serial dilutions were prepared to make 2 mM, 400 μM, 80 μM, 16 μM, and 3.2 μM peptide stock solutions. Ten-fold serial dilutions were prepared to make 1 mM, 100 μM, 10 μM, 1 μM, and 0.1 μM peptide stock solutions. For each peptide dilution, a 15 μL volume was transferred to 585 μL of EphB2-Fc stock solution (described above) and mixed gently to produce solutions containing EphB2-Fc and peptide concentrations from 2.5 nM to 250 μM.

Step 2: After washing, a 200 μL volume of each EphB2−peptide mixture was added to triplicate wells. A negative control without EphB2 was also added to the plate by adding 200 μL of TBST to triplicate wells. A positive control was also added to the plate by adding 200 μL of peptide-free EphB2-Fc to triplicate wells (peptide-free EphB2-Fc = 15 μL water added to 585 μL EphB2-Fc stock solution). The plate was covered in parafilm and incubated overnight at 4 °C.

Step 3: After washing, a 200 μL volume of antihuman IgG stock solution was added to each sample well. The plate was covered with parafilm and incubated for 1 h with mild shaking (150 rpm) on an orbital shaker at RT.

Step 4: Immediately prior to washing, the pNPP solution was prepared by dissolving 5 mg of pNPP in 5 mL of 1× diethanolamine (DEA) buffer. After washing, a 100 μL volume of pNPP stock solution was added to each well. The absorbance of each sample well at 405 nm was measured using a 96-well plate reader at 15 min intervals for 2 h.

To obtain $IC_{50}$ values, absorbance data for triplicate samples at each time point were averaged. Peptide-containing samples were normalized as follows:

$$\text{Normalized absorbance} = 100 \times \frac{A_{405}(\text{sample}) - A_{405}(-)}{A_{405}(+) - A_{405}(-)}$$

where $A_{405}(-)$ is the average absorbance for the triplicate negative control samples (i.e., no EphB2-Fc or peptide added) and $A_{405}(+)$ is the average absorbance for the triplicate positive control samples (i.e., EphB2-Fc added but no peptide). All ELISAs were performed at least twice and averaged for data fitting. $IC_{50}$ values were obtained by fitting the data to the following three-parameter equation:

$$y = \frac{100}{1 + \frac{x}{IC_{50}}}$$

where $x$ is the peptide concentration, $y$ is the normalized absorbance, and $IC_{50}$ is the $IC_{50}$ value.



https://doi.org/10.1021/acschembio.3c00791
ACS Chem. Biol. 2024, 19, 1214−1221

**Circular Dichroism Spectroscopy.** Circular dichroism spectra were acquired using a Jasco J-1500 CD spectrometer at a concentration of 30 $\mu$M in 10 mM sodium phosphate (pH 7.6) in a 0.1 cm path length cell.

**Nuclear Magnetic Resonance (NMR) Spectroscopy and Molecular Modeling.** Experiments were performed on a Bruker 800 MHz NMR spectrometer. Peptides **29** and **30** were dissolved in 20 mM sodium phosphate buffer at pH 4.7 to a concentration of 1 mM. One-dimensional $^1$H, 2D TOCSY, 2D NOESY, and 2D ROESY spectra were acquired using solvent suppression (zgesgp, mlevesgpph, noesyesgpph, and roesyesgpph pulse sequences, respectively). TOCSY and NOESY mixing times were 80 and 120 ms, respectively. Spectral data were processed using Bruker TOPSPIN. Resonances were assigned using TOCSY and NOESY data and are reported in Table S3. Coupling constants ($^3J_{NHC\alpha H}$) were determined using the 1D $^1$H data and used to calculate $\varphi$ dihedral angle values using the Pardi parameterized Karplus equation,[45] both of which are reported in Table S3. NOE cross-peaks are reported in Table S4.

To generate conformational ensembles for peptides **29** and **30**, a starting structure for molecular modeling was constructed based on the isolated QPRL region at the C-terminus of the SNEW peptide (PDB 2QBX)[14] with an acetylated N-terminus and amidated C-terminus. Using the PyMOL Mutagenesis tool, Gln and Leu residues were mutated to cysteine and either manually cross-linked with a 2,7-dimethylnaphthyl group (**29**) or modified with one benzyl group per cysteine (**30**). Dihedral angle constraints were introduced based on the calculated $\varphi$ dihedral angles (±15°). Distance constraints were introduced for each NOE cross-peak for **29** based on peak strength: 3.0 ± 1.0 Å for strong cross-peaks, 4.0 ± 1.0 Å for medium cross-peaks, and 4.5 ± 1.0 Å for weak cross-peaks. Monte Carlo conformational searches for peptides **29** and **30** were performed using the OPLS_2005 force field with mixed torsional and low-mode sampling. A total of three dihedral angle constraints and 18 distance constraints were used for **29** to constrain a Monte Carlo conformational search in the Macromodel program. The 20 lowest energy structures for **29** show high peptide backbone convergence, while the 20 lowest energy structures for **30** showed only moderate peptide backbone convergence. Conformational ensembles for these structures are reported in Figures 4B and S12.

**Determining EphB Receptor Specificity.** ELISAs to determine Eph receptor binding specificity were performed as described in the competitive ELISA procedure except for step 2. For step 2, stock solutions for each EphB receptor were prepared as described for EphB2 in the competitive ELISA procedure. From a 10 mM peptide stock solution in water, a 2 mM peptide solution was prepared by 5-fold dilution in water. For each EphB receptor, a volume of 15 $\mu$L of 2 mM peptide was added to 585 $\mu$L of the EphB receptor stock solution before addition to the 96-well plate. For each EphB receptor, a matched sample without peptide (15 $\mu$L of water in 585 $\mu$L EphB receptor) was also prepared as a receptor-specific positive control. Each of these mixtures was added to triplicate wells. As a negative control, 200 $\mu$L of TBST was added to each triplicate well at this step. All ELISAs were performed at least twice and averaged. Data were normalized as described for the competitive ELISA procedure.

**Trypsin Digestion.** To analyze trypsin proteolysis for each peptide, a volume of 150 $\mu$L of peptide solution was prepared at 300 $\mu$M. This volume was equally distributed into three 50 $\mu$L samples. To each sample, 200 $\mu$L of sodium phosphate buffer, at pH 7.4, and 50 $\mu$L of 0.12 $\mu$M trypsin were added sequentially. After gentle mixing, samples were added to a 37 °C water bath for defined time intervals. After incubation, samples were quenched by adding 60 $\mu$L of ice-cold aqueous trichloroacetic acid (15% w/v). For each peptide, a negative control sample at $t$ = 0 was prepared by adding the trichloroacetic acid before adding trypsin. The percentage of peptide remaining after each time interval was determined by integration of HPLC chromatograms for each sample.

## ■ ASSOCIATED CONTENT

### Supporting Information

The Supporting Information is available free of charge at https://pubs.acs.org/doi/10.1021/acschembio.3c00791.

800 MHz CPRC conformational ensemble (ZIP)

Computational alanine scanning data, analysis of $\alpha$-helical cross-linkers, synthetic schemes for cross-linked peptides, ELISA data, $^1$H NMR data, trypsin digestion data, analytical HPLC data, and additional experimental details (PDF)

## ■ AUTHOR INFORMATION


### Corresponding Author

**Nicholas Sawyer** − *Department of Chemistry, Fordham University, Bronx, New York 10458, United States;* orcid.org/0000-0002-6393-5626; Email: nsawyer@fordham.edu

### Authors

**Jessica C. Tennett** − *Department of Chemistry, Fordham University, Bronx, New York 10458, United States*

**Sophie R. Epstein** − *Department of Chemistry, Fordham University, Bronx, New York 10458, United States*

Complete contact information is available at: https://pubs.acs.org/10.1021/acschembio.3c00791


### Notes

The authors declare no competing financial interest.

## ■ ACKNOWLEDGMENTS

We thank P. Arora and J. Ongkingco at New York University for assistance with molecular dynamics simulations and C. Lin at New York University for assistance with NMR experiments. J.C.T. thanks the Clare Boothe Luce Program and Fordham College Dean's Office for funding support. S.R.E. thanks the Fordham College Dean's Office for funding support. N.S. thanks Fordham University for start-up funding and faculty research grant support.

## ■ REFERENCES

(1) Lemmon, M. A.; Schlessinger, J. Cell Signaling by Receptor Tyrosine Kinases. *Cell* **2010**, *141*, 1117−1134.

(2) Eph Nomenclature Committee. Unified Nomenclature for Eph Family Receptors and Their Ligands, the Ephrins. *Cell* **1997**, *90*, 403−404.

(3) Pasquale, E. B. The Eph family of receptors. *Curr. Opin. Cell Biol.* **1997**, *9*, 608−615.

(4) Cheng, N.; Brantley, D. M.; Chen, J. The ephrins and Eph receptors in angiogenesis. *Cytokine Growth Factor Rev.* **2002**, *13*, 75−85.

(5) Easty, D. J.; Herlyn, M.; Bennett, D. C. Abnormal protein tyrosine kinase gene expression during melanoma progression and metastasis. *Int. J. Cancer* **1995**, *60*, 129−136.

(6) Mao, W.; Luis, E.; Ross, S.; Silva, J.; Tan, C.; Crowley, C.; Chui, C.; Franz, G.; Senter, P.; Koeppen, H.; Polakis, P. EphB2 as a Therapeutic Antibody Drug Target for the Treatment of Colorectal Cancer. *Cancer Res.* **2004**, *64*, 781−788.

(7) Blits-Huizinga, C. T.; Nelersa, C. M.; Malhotra, A.; Liebl, D. J. Ephrins and their Receptors: Binding versus Biology. *IUBMB Life* **2004**, *56*, 257−265.

(8) Himanen, J.-P.; Chumley, M. J.; Lackmann, M.; Li, C.; Barton, W. A.; Jeffrey, P. D.; Vearing, C.; Geleick, D.; Feldheim, D. A.; Boyd, A. W.; Henkemeyer, M.; Nikolov, D. B. Repelling class discrim-

ination: ephrin-A5 binds to and activates EphB2 receptor signaling. *Nat. Neurosci.* **2004**, *7*, 501−509.
(9) Boyd, A. W.; Bartlett, P. F.; Lackmann, M. Therapeutic targeting of EPH receptors and their ligands. *Nat. Rev. Drug Discov.* **2014**, *13*, 39−62.
(10) Barquilla, A.; Pasquale, E. B. Eph Receptors and Ephrins: Therapeutic Opportunities. *Annu. Rev. Pharmacol. Toxicol.* **2015**, *55*, 465−487.
(11) Koolpe, M.; Dail, M.; Pasquale, E. B. An Ephrin Mimetic Peptide That Selectively Targets the EphA2 Receptor*. *J. Biol. Chem.* **2002**, *277*, 46974−46979.
(12) Murai, K. K.; Nguyen, L. N.; Koolpe, M.; McLennan, R.; Krull, C. E.; Pasquale, E. B. Targeting the EphA4 receptor in the nervous system with biologically active peptides. *Mol. Cell. Neurosci.* **2003**, *24*, 1000−1011.
(13) Koolpe, M.; Burgess, R.; Dail, M.; Pasquale, E. B. EphB Receptor-binding Peptides Identified by Phage Display Enable Design of an Antagonist with Ephrin-like Affinity. *J. Biol. Chem.* **2005**, *280*, 17301−17311.
(14) Chrencik, J. E.; Brooun, A.; Recht, M. I.; Nicola, G.; Davis, L. K.; Abagyan, R.; Widmer, H.; Pasquale, E. B.; Kuhn, P. Three-dimensional Structure of the EphB2 Receptor in Complex with an Antagonistic Peptide Reveals a Novel Mode of Inhibition. *J. Biol. Chem.* **2007**, *282*, 36505−36513.
(15) Sawyer, N.; Watkins, A. M.; Arora, P. S. Protein Domain Mimics as Modulators of Protein-Protein Interactions. *Acc. Chem. Res.* **2017**, *50*, 1313−1322.
(16) Lau, Y. H.; de Andrade, P.; Wu, Y.; Spring, D. R. Peptide stapling techniques based on different macrocyclisation chemistries. *Chem. Soc. Rev.* **2015**, *44*, 91−102.
(17) Peraro, L.; Siegert, T. R.; Kritzer, J. A. Chapter Fourteen - Conformational Restriction of Peptides Using Dithiol Bis-Alkylation. In *Methods in Enzymology*; Pecoraro, V. L., Ed.; Academic Press, 2016; Vol. *580*, pp 303−332.
(18) Horng, J.-C.; Raines, R. T. Stereoelectronic effects on polyproline conformation. *Protein Sci.* **2006**, *15*, 74−83.
(19) Kümin, M.; Sonntag, L.-S.; Wennemers, H. Azidoproline Containing Helices: Stabilization of the Polyproline II Structure by a Functionalizable Group. *J. Am. Chem. Soc.* **2007**, *129*, 466−467.
(20) Brown, A. M.; Zondlo, N. J. A Propensity Scale for Type II Polyproline Helices (PPII): Aromatic Amino Acids in Proline-Rich Sequences Strongly Disfavor PPII Due to Proline−Aromatic Interactions. *Biochemistry* **2012**, *51*, 5041−5051.
(21) Pandey, A. K.; Naduthambi, D.; Thomas, K. M.; Zondlo, N. J. Proline Editing: A General and Practical Approach to the Synthesis of Functionally and Structurally Diverse Peptides. Analysis of Steric versus Stereoelectronic Effects of 4-Substituted Prolines on Conformation within Peptides. *J. Am. Chem. Soc.* **2013**, *135*, 4333−4363.
(22) Rajewski, B. H.; Wright, M. M.; Gerrein, T. A.; Del Valle, J. R. N-Aminoglycine and Its Derivatives Stabilize PPII Secondary Structure. *Org. Lett.* **2023**, *25*, 4366−4370.
(23) Luong, H. X.; Kim, Y.-W. Stabilization of Single Turn Polyproline II Helices via Macrocyclic Hydrocarbon Staples. *Org. Lett.* **2020**, *22*, 7986−7990.
(24) Tseng, W.-H.; Li, M.-C.; Horng, J.-C.; Wang, S.-K. Strategy and Effects of Polyproline Peptide Stapling by Copper(I)-Catalyzed Alkyne−Azide Cycloaddition Reaction. *ChemBioChem.* **2019**, *20*, 153−158.
(25) Merritt, H. I.; Sawyer, N.; Arora, P. S. Bent into shape: Folded peptides to mimic protein structure and modulate protein function. *Peptide Sci.* **2020**, *112*, No. e24145.
(26) Yu, H.; Chen, J. K.; Feng, S.; Dalgarno, D. C.; Brauer, A. W.; Schrelber, S. L. Structural basis for the binding of proline-rich peptides to SH3 domains. *Cell* **1994**, *76*, 933−945.
(27) Pawson, T.; Nash, P. Assembly of Cell Regulatory Systems Through Protein Interaction Domains. *Science* **2003**, *300*, 445−452.
(28) Rath, A.; Davidson, A. R.; Deber, C. M. The structure of "unstructured" regions in peptides and proteins: Role of the polyproline II helix in protein folding and recognition*. *Peptide Sci.* **2005**, *80*, 179−185.
(29) Wood, C. W.; Ibarra, A. A.; Bartlett, G. J.; Wilson, A. J.; Woolfson, D. N.; Sessions, R. B. BAlaS: fast, interactive and accessible computational alanine-scanning using BudeAlaScan. *Bioinformatics* **2020**, *36*, 2917−2919.
(30) Shepherd, N. E.; Hoang, H. N.; Abbenante, G.; Fairlie, D. P. Single Turn Peptide Alpha Helices with Exceptional Stability in Water. *J. Am. Chem. Soc.* **2005**, *127*, 2974−2983.
(31) de Araujo, A. D.; Hoang, H. N.; Kok, W. M.; Diness, F.; Gupta, P.; Hill, T. A.; Driver, R. W.; Price, D. A.; Liras, S.; Fairlie, D. P. Comparative $\alpha$-Helicity of Cyclic Pentapeptides in Water. *Angew. Chem., Int. Ed.* **2014**, *53*, 6965−6969.
(32) Schafmeister, C. E.; Po, J.; Verdine, G. L. An All-Hydrocarbon Cross-Linking System for Enhancing the Helicity and Metabolic Stability of Peptides. *J. Am. Chem. Soc.* **2000**, *122*, 5891−5892.
(33) Walensky, L. D.; Bird, G. H. Hydrocarbon-Stapled Peptides: Principles, Practice, and Progress. *J. Med. Chem.* **2014**, *57*, 6275−6288.
(34) Jo, H.; Meinhardt, N.; Wu, Y.; Kulkarni, S.; Hu, X.; Low, K. E.; Davies, P. L.; DeGrado, W. F.; Greenbaum, D. C. Development of $\alpha$-Helical Calpain Probes by Mimicking a Natural Protein−Protein Interaction. *J. Am. Chem. Soc.* **2012**, *134*, 17704−17713.
(35) Fujimoto, K.; Kajino, M.; Inouye, M. Development of a Series of Cross-Linking Agents that Effectively Stabilize $\alpha$-Helical Structures in Various Short Peptides. *Chem. Eur. J.* **2008**, *14*, 857−863.
(36) Adzhubei, A. A.; Sternberg, M. J. E.; Makarov, A. A. Polyproline-II Helix in Proteins: Structure and Function. *J. Mol. Biol.* **2013**, *425*, 2100−2132.
(37) Liu, F.; Giubellino, A.; Simister, P. C.; Qian, W.; Giano, M. C.; Feller, S. M.; Bottaro, D. P.; Burke, T. R., Jr Application of ring-closing metathesis to Grb2 SH3 domain-binding peptides. *Peptide Sci.* **2011**, *96*, 780−788.
(38) Chandra, K.; Naoum, J. N.; Roy, T. K.; Gilon, C.; Gerber, R. B.; Friedler, A. Mechanistic studies of malonic acid-mediated in situ acylation. *Peptide Sci.* **2015**, *104*, 495−505.
(39) Kale, S. S.; Villequey, C.; Kong, X.-D.; Zorzi, A.; Deyle, K.; Heinis, C. Cyclization of peptides with two chemical bridges affords large scaffold diversities. *Nat. Chem.* **2018**, *10*, 715−723.
(40) Wulff, G.; Krieger, S.; Kuehneweg, B.; Steigel, A. Occurrence of strong circular dichroism during measurement of CD spectra due to intramolecular cyclization. *J. Am. Chem. Soc.* **1994**, *116*, 409−410.
(41) Chen, L.; Morris, K.; Laybourn, A.; Elias, D.; Hicks, M. R.; Rodger, A.; Serpell, L.; Adams, D. J. Self-Assembly Mechanism for a Naphthalene−Dipeptide Leading to Hydrogelation. *Langmuir* **2010**, *26*, 5232−5242.
(42) Di Bari, L.; Pescitelli, G.; Salvadori, P. Conformational Study of 2,2′-Homosubstituted 1,1′-Binaphthyls by Means of UV and CD Spectroscopy. *J. Am. Chem. Soc.* **1999**, *121*, 7998−8004.
(43) Stringer, J. R.; Crapster, J. A.; Guzei, I. A.; Blackwell, H. E. Extraordinarily Robust Polyproline Type I Peptoid Helices Generated via the Incorporation of $\alpha$-Chiral Aromatic N-1-Naphthylethyl Side Chains. *J. Am. Chem. Soc.* **2011**, *133*, 15559−15567.
(44) Wang, Y.; Nip, A. M.; Wishart, D. S. A simple method to quantitatively measure polypeptide JHNH$\alpha$ coupling constants from TOCSY or NOESY spectra. *J. Biomol. NMR* **1997**, *10*, 373−382.
(45) Pardi, A.; Billeter, M.; Wüthrich, K. Calibration of the angular dependence of the amide proton-C$\alpha$ proton coupling constants, 3JHN$\alpha$, in a globular protein: Use of 3JHN$\alpha$ for identification of helical secondary structure. *J. Mol. Biol.* **1984**, *180*, 741−751.
(46) Nguyen, J. T.; Turck, C. W.; Cohen, F. E.; Zuckermann, R. N.; Lim, W. A. Exploiting the Basis of Proline Recognition by SH3 and WW Domains: Design of N-Substituted Inhibitors. *Science* **1998**, *282*, 2088−2092.
(47) Zarrinpar, A.; Bhattacharyya, R. P.; Lim, W. A. The Structure and Function of Proline Recognition Domains. *Sci. Signal.* **2003**, *2003*, re8.


https://doi.org/10.1021/acschembio.3c00791
*ACS Chem. Biol.* 2024, 19, 1214−1221